A

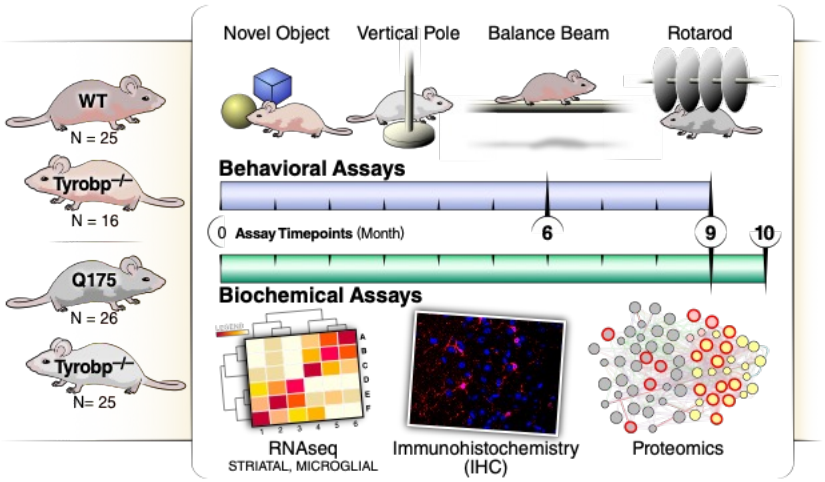


B

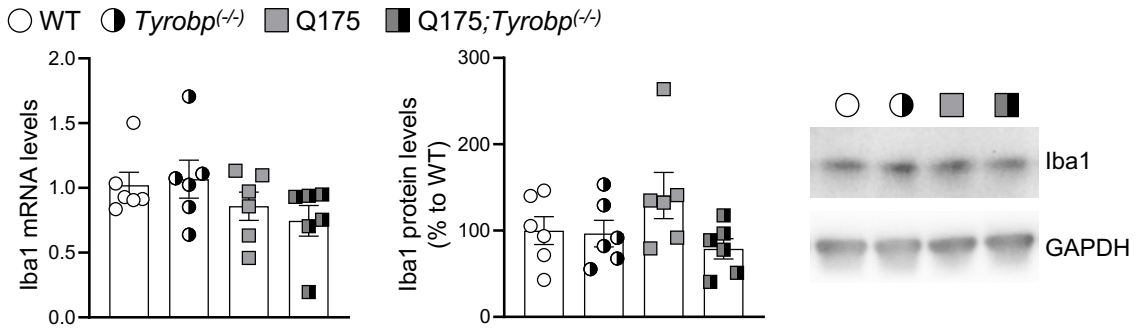


**Supplementary Fig. 1.** (A) Schematic of the biochemical and behavioral studies on WT and Q175 mice with and without *Tyrobp*. (B) RT-qPCR of *Aif1* (Iba1 gene) mRNA (left) and WB of Iba1 protein (right) in the striatum of WT and Q175 mice with and without *Tyrobp* (10 months of age), n = 6 mice per group. Each point represents data from an individual mouse.

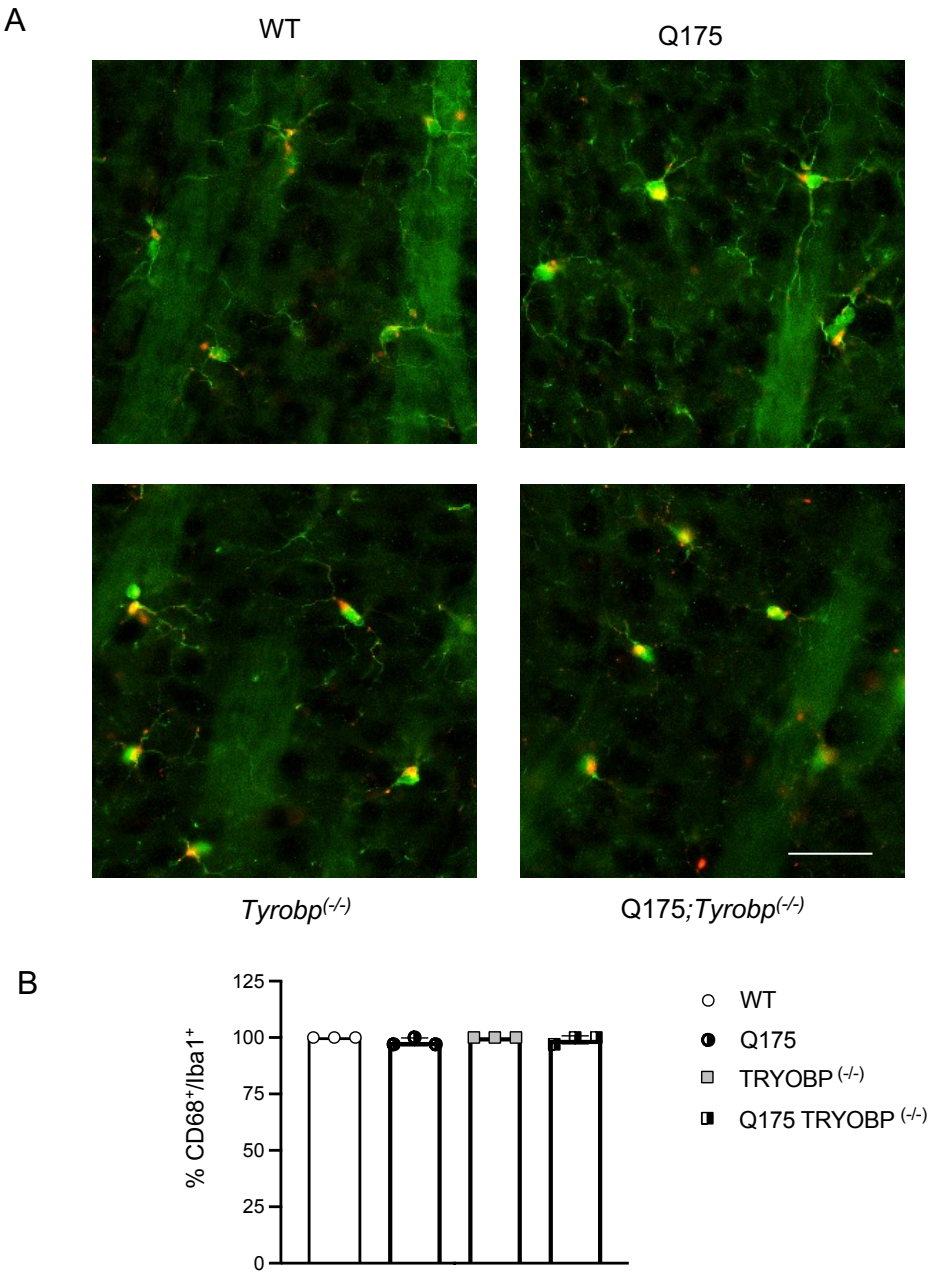


**Supplementary Fig. 2.** (A) Representative immunofluorescent images of of CD68 cells colabeled with Iba1. Virtually all cells were double-labeled in all genotypes. (B) Quantification of the $CD68^+$ cells were positive for $Iba1^+$ cells. Averaged number of $CD68^+$ cells were positive for $Iba1^+$ cells from three fields from 3 different striatal sections is represented per group as mean ± SEM (WT n= 3; Q175 n = 3; $Tyrobp^{(-/-)}$ n= 3 Q175;$Tyrobp^{(-/-)}$ n = 3). Each point represents data from an individual mouse. Scale bar = 5 μm.

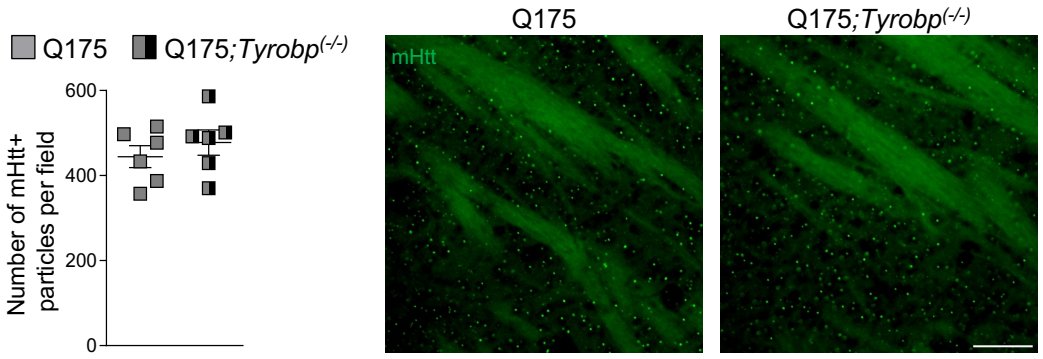


**Supplementary Fig. 3.** Number of mHtt+ particles was evaluated in the dorsal striatum of Q175 mice at 9 months of age. Averaged number of mHtt+ particles from four fields from 3 different striatal sections is represented per group as mean ± SEM (Q175 n = 6; Q175;Tyrobp(-/-) n = 6). Each point represents data from an individual mouse. Scale bar = 50 μm.

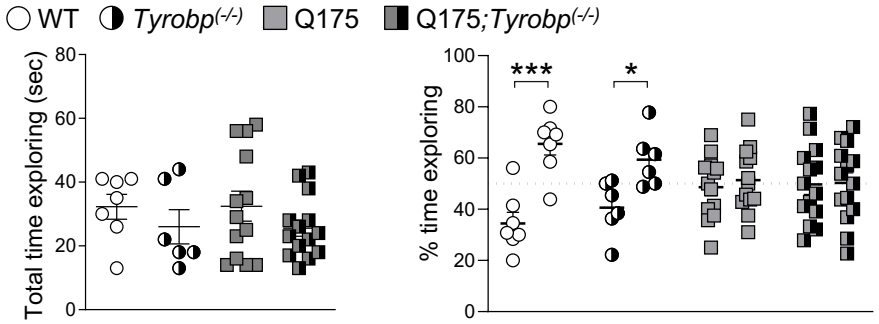


**Supplementary Fig. 4.** Cognitive behavior was evaluated in Q175 mice at 9 months of age using the Novel Object Recognition test (NOR). Time exploring and percentage exploring each arm is represented per group as mean ± SEM (WT n = 7; Tyrobp(-/-) n = 6; Q175 n = 13; Q175;Tyrobp(-/-) = 14). Each point represents data from an individual mouse. Statistical analysis was performed unpaired t-test comparing old vs new arm. *p < 0.05; ***p < 0.001.

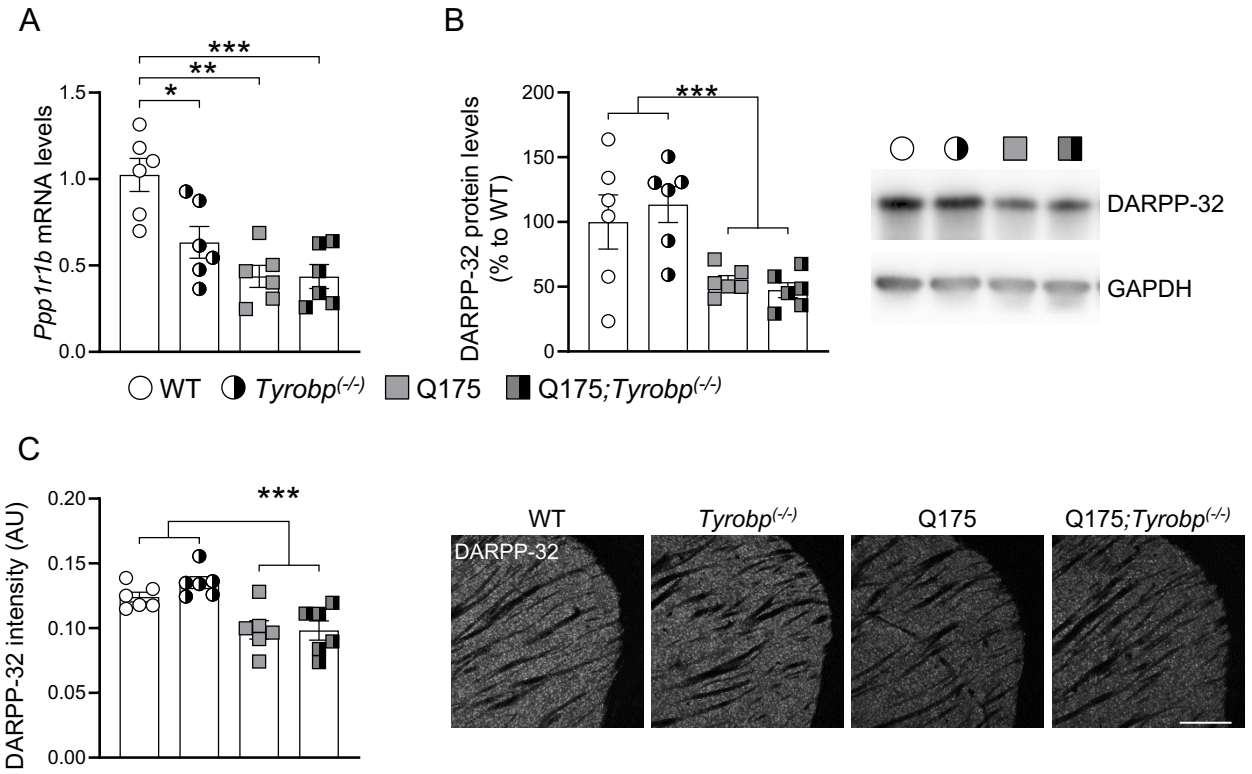


**Supplementary Fig. 5.** (A) RT-qPCR, (B) WB and (C) immunofluorescence analysis of DARPP-32 in the striatum of WT and Q175 mice with and without *Tyrobp* (10 months of age), n = 6 mice per group. Data represent the mean ± SEM. Each point represents data from an individual mouse. Two-way ANOVA followed by Bonferroni's post hoc test, *p < 0.05; **p < 0.01; ***p < 0.001. Scale bar = 200 μm.

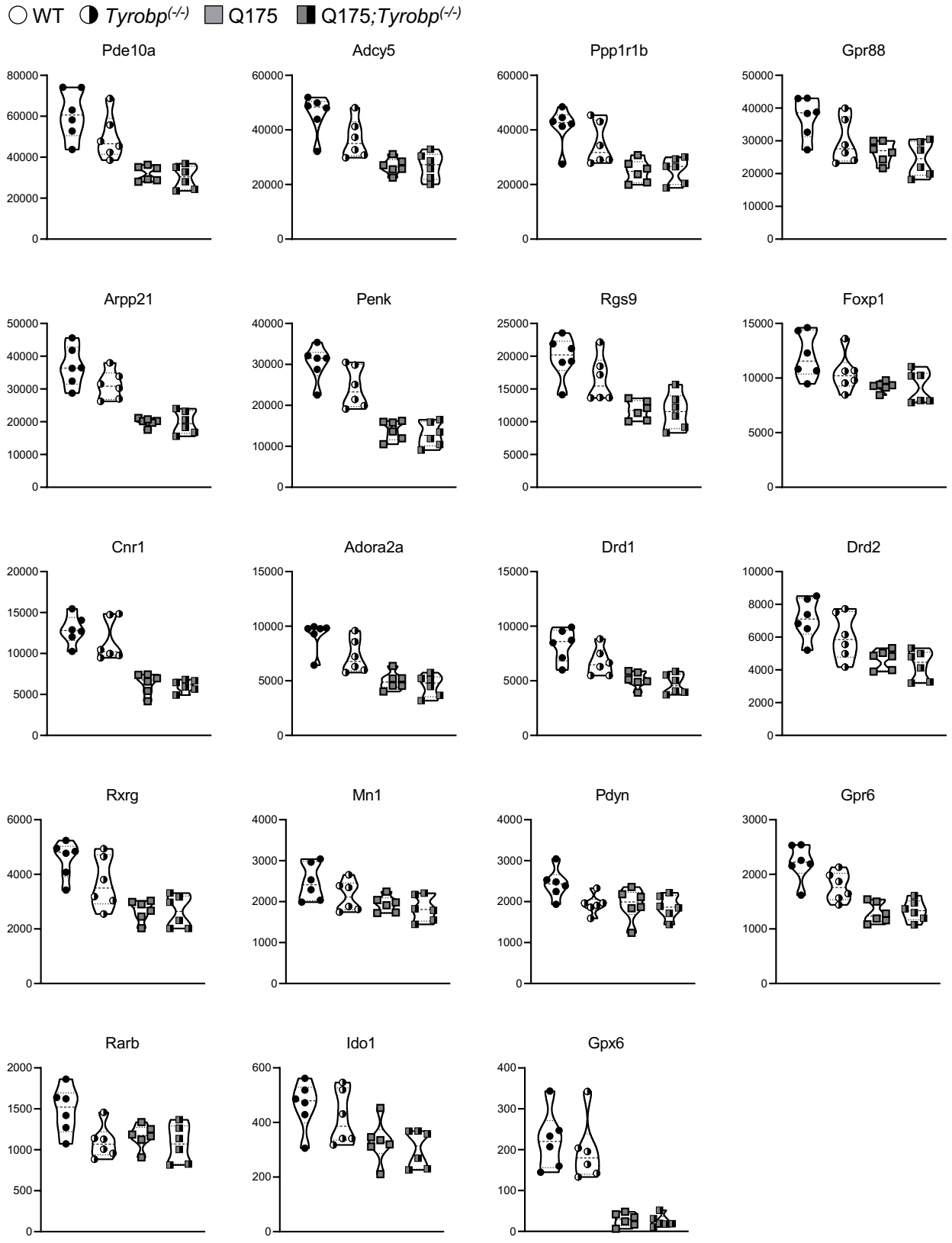


**Supplementary Fig. 6**. Normalized counts of striatal-specific genes detected in the striatum of WT and Q175 mice with and without Tyrobp (10 months of age) by bulk RNAseq, n = 6 mice per group.

A

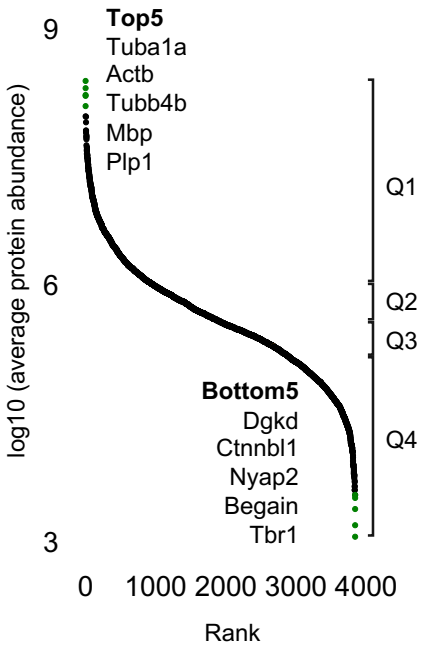


B

| Quartile | GO Biological Process 2021 | FDR | OR |
|---|---|---|---|
| Q1: | aerobic electron transport chain | 1.403E-35 | 33.1 |
| Q2: | cytoplasmic translation | 1.677E-22 | 14.26 |
| Q3: | post-Golgi vesicle-mediated transport | 4.992E-07 | 6.63 |
| Q4: | mitochondrial translational elongation | 2.689E-10 | 7.94 |

| Quartile | GO Cellular Component 2021 | FDR | OR |
|---|---|---|---|
| Q1: | focal adhesion | 2.217E-51 | 8.67 |
| Q2: | cytosolic large ribosomal subunit | 5.144E-14 | 14.61 |
| Q3: | late endosome | 3.342E-07 | 3.98 |
| Q4: | mitochondrial inner membrane | 0.0001579 | 2.67 |

**Supplementary Fig. 7**. (A) Ranking of brain proteins by normalized protein abundance from highest to lowest. (B) Top enrichment for each quartile is displayed for GO categories “biological process” and “cellular component”; FDR, Benjamini-Hochberg-corrected false discovery rate. OR, Odds Ratio.

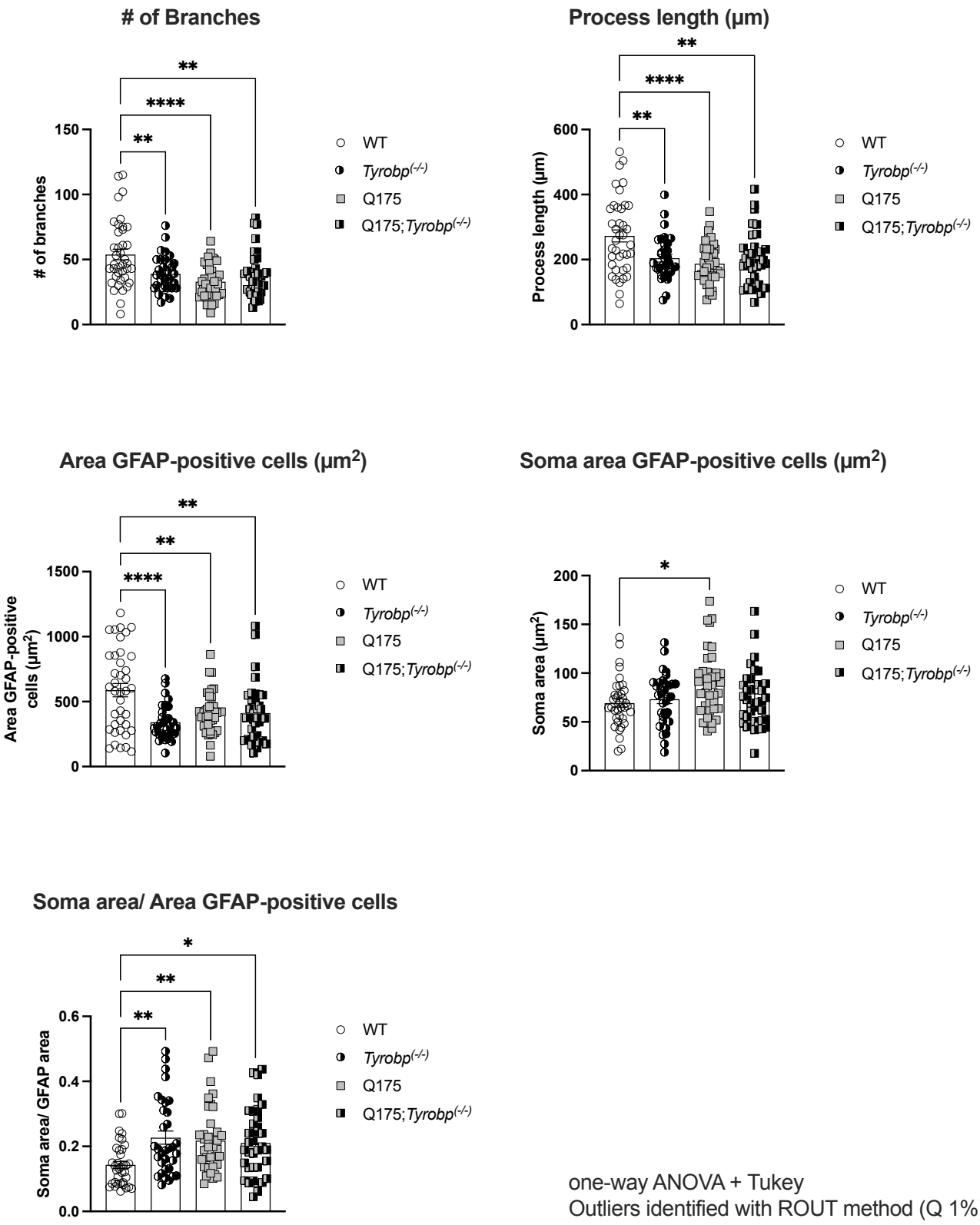


**Supplementary Fig. 8.** Quantification of the morphology of GFAP cells in the striatum of WT and Q175 mice with and without *Tyrobp*.